HUMAN EVOLUTION

Extreme glacial cooling likely led to hominin depopulation of Europe in the Early Pleistocene

Vasiliki Margari[1], David A. Hodell[2], Simon A. Parfitt[3,4], Nick M. Ashton[5], Joan O. Grimalt[6], Hyuna Kim[7,8], Kyung-Sook Yun[7,9], Philip L. Gibbard[10], Chris B. Stringer[4], Axel Timmermann[7,9]*, Polychronis C. Tzedakis[1]*

The oldest known hominin remains in Europe [~1.5 to ~1.1 million years ago (Ma)] have been recovered from Iberia, where paleoenvironmental reconstructions have indicated warm and wet interglacials and mild glacials, supporting the view that once established, hominin populations persisted continuously. We report analyses of marine and terrestrial proxies from a deep-sea core on the Portugese margin that show the presence of pronounced millennial-scale climate variability during a glacial period ~1.154 to ~1.123 Ma, culminating in a terminal stadial cooling comparable to the most extreme events of the last 400,000 years. Climate envelope–model simulations reveal a drastic decrease in early hominin habitat suitability around the Mediterranean during the terminal stadial. We suggest that these extreme conditions led to the depopulation of Europe, perhaps lasting for several successive glacial-interglacial cycles.

The earliest published fossil hominin (*Homo* sp.) evidence in Europe is a mandible and a hand phalanx found with stone tools at the site of Sima del Elefante, Sierra de Atapuerca, northern Spain (*1*, *2*), as well as a deciduous molar and stone tools from the sites of Barranco León and Fuente Nueva 3, Guadix-Baza Basin, southeastern Spain (*3*, *4*). Analysis of traits of the Sima del Elefante hominin suggests a possible Eurasian (rather than African) evolutionary origin (*5*) for the population that it represents. Given that hominins were present at Dmanisi, Georgia, ~1.8 million years ago (Ma) (*6*), dispersal into Europe could have taken place at any time after that, but sites in Italy and Spain yielding stone tools and human remains over a broad time window of ~1.6 to ~1.1 Ma indicate a delay of ~200 thousand years (kyr) (Fig. 1 and table S1) (*7*). This dispersal lag may be attributed to a period of cooler interglacials ~1.8 to ~1.6 Ma, which in turn may be related to the 1.2-million-year (Myr) amplitude modulation of the obliquity cycle (*8*).

Considerable disagreement remains on whether early hominin occupation was permanent (*9*–*11*) or restricted to interglacials, implying that southern Europe was repeatedly colonized from Southwest Asia (*12*–*14*). Although various factors (geographical, biological, technocultural, and demographic) influence hominin occupation patterns, environmental conditions ultimately act as a limiting factor. Therefore, reconstructions of the climatic backgroun… hominin occupation can constrain the li… hood of different scenarios.

Before 1.2 Ma, glacial-interglacial cycles occurred with a period of ~41 kyr, with maximum ice volumes ranging between one-half and one-third of the Last Glacial Maximum value (*15*, *16*). The less-extensive ice sheets and shorter glacial periods of the Early Pleistocene have been linked to smaller decreases in temperature compared with those of the Middle and Late Pleistocene. Nonetheless, North Atlantic records point to the occurrence of iceberg discharges from marine-terminating ice sheets and disruptions of the Atlantic meridional overturning circulation (AMOC) during the interval ~1.43 to ~1.25 Ma (*17*–*20*), but their downstream impacts on European climate remain largely unknown. A lengthening and intensification of glacial-interglacial cycles took place over the so-called Early-Middle Pleistocene Transition [~1.25 to ~0.70 Ma (*21*)], after which ice volume varied with a dominant ~80- to ~120-kyr periodicity.

Paleoenvironmental reconstructions based on animal and plant remains from the Atapuerca and Guadix-Baza occupation levels indicate a diverse mosaic of Mediterranean and temperate woodlands, open shrublands, and extensive

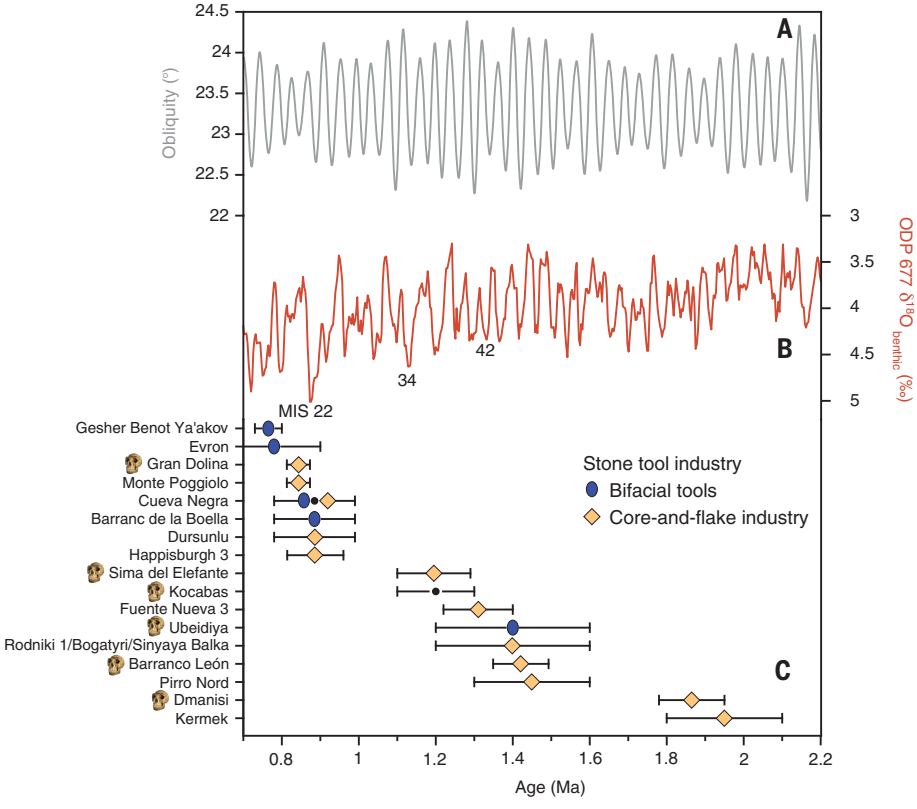

Fig. 1. Age estimates of European and Southwest Asian early hominin sites and paleoclimate context. (**A**) Obliquity variations (*60*). (**B**) Benthic oxygen isotope record from eastern equatorial Pacific Site ODP677 (*15*). (**C**) Age estimates of European and Southwest Asian early hominin sites (table S1). Stone-tool industries are shown; sites with hominin remains are indicated by skulls. Site selection is based on presence of human remains, strong evidence of humanly manufactured lithic artifacts, and a secure chronological framework (*7*).

[1]Environmental Change Research Centre, Department of Geography, University College London, London WC1E 6BT, UK. [2]Department of Earth Sciences, University of Cambridge, Cambridge CB2 3EQ, UK. [3]Institute of Archaeology, University College London, London WC1H 0PY, UK. [4]Centre for Human Evolution Research, The Natural History Museum, London SW7 5BD, UK. [5]Department of Britain, Europe and Prehistory, British Museum, London N1 5QJ, UK. [6]Department of Environmental Chemistry, Institute of Environmental Assessment and Water Research (IDAEA), Spanish Council for Scientific Research (CSIC), 08034 Barcelona, Spain. [7]Institute for Basic Science, Center for Climate Physics, Busan 46241, South Korea. [8]Department of Climate System, Pusan National University, Busan 46241, South Korea. [9]Pusan National University, Busan 46241, South Korea. [10]Scott Polar Research Institute, University of Cambridge, Cambridge CB2 1ER, UK.
*Corresponding author. Email: p.c.tzedakis@ucl.ac.uk (P.C.T.); axel@ibsclimate.org (A.T.)

wetlands, with mean annual temperatures similar to those of the present, but higher mean annual precipitation (*10*, *22*–*25*). The presence of thermophilous species within a mosaic of woodland and open habitats throughout the Sima del Elefante sequence has been used to infer relative ecological stability during both interglacials and glacials and to argue for the continuity of occupation (*10*), but stratigraphical hiatuses and preservation biases may have led to intermittent representation, complicating such interpretations. Early Pleistocene pollen sequences are available from northeastern Spain (*26*) but are fragmentary and lack precise chronologies. In the Guadix-Baza Basin, the Palominas pollen record contains a succession of ~10 forest and open-vegetation phases, representing interglacial and glacial periods, respectively (*27*). In the absence of independent chronological controls, biostratigraphical correlations point to the record extending from ~1.6 to ~1.2 Ma (*27*). Pollen-based climate reconstructions suggest that mean annual precipitation levels during glacials were similar to modern levels and higher during interglacials; temperature reconstructions for both glacials and interglacials indicate values similar to those of the present (*27*). The implication is that these conditions would have allowed hominin populations to persist through glacials and expand during interglacials (*11*).

Assessing climate impacts on human populations

To address the pervasive issues with stratigraphical continuity and chronological control in terrestrial sedimentary sequences, we have undertaken an examination of the paleoenvironmental context during the interval of early human occupation at deep-sea Site U1385 on the southwestern Portuguese margin (*28*) (fig. S1), a prime location for joint marine-terrestrial analyses and correlations (*29*–*32*). Sites on the southwestern Portuguese margin are also well situated to record past changes in North Atlantic surface and deep-ocean circulation: During Marine Isotope Stage (MIS) 3 [59 to 24 thousand years ago (ka)], the oxygen isotopic composition of planktic foraminifera ($\delta^{18}O_{planktic}$) closely matched the Greenland temperature record, with abrupt transitions marking the onset and end of interstadials, whereas the oxygen isotopic composition of benthic foraminifera ($\delta^{18}O_{benthic}$) resembled the Antarctic temperature record, both in its shape and phasing relative to Greenland (*33*). This asynchronous phasing between $\delta^{18}O_{planktic}$ and $\delta^{18}O_{benthic}$ has been interpreted as a fingerprint of AMOC changes associated with interhemispheric heat transport and the bipolar seesaw (*31*). Here, we focus on reconstructing sea and land changes during two time windows of the interval of early hominin occupation, representing distinct climatic contexts: a 41-kyr cycle, MIS 43 to 42 (~1.380 to ~1.338 Ma), and one cycle from the Early-Middle Pleistocene Transition, MIS 35 to 34 (~1.192 to ~1.123 Ma). Analyses (*7*) were undertaken with respect to (i) $\delta^{18}O_{planktic}$ and $\delta^{18}O_{benthic}$, reflecting changes in surface-water conditions, and in global ice-volume and deep-water hydrography, respectively; (ii) the relative composition of C37 unsaturated alkenones, reflecting surface-water conditions; (iii) pollen content, providing an integrated picture of regional vegetation changes in southwestern Portugal; and (iv) x-ray fluorescence (XRF) sediment-composition changes, reflecting variations in the relative proportion of detrital (Zr) and biogenic (Sr) sediment supply.

To assess and further quantify the climate impact on human occupation, we developed a climate envelope model that is based on climate data from a 2-Myr transient coupled general circulation model simulation (*34*) and a new database of early hominin sites for Europe and Southwest Asia (table S1) (*7*). This model, which calculates hominin habitat suitability as a function of net primary productivity and minimum annual temperature, was then forced with the respective climate data obtained from a freshwater perturbation model experiment (*7*).

Paleoenvironmental reconstructions

Figure 2 (right) shows the results of our analyses for the interval MIS 43 to 42. The onset of warm conditions occurred at ~1.380 Ma, marked by a decrease in detrital sediment supply and a shift to higher alkenone-based sea surface temperature (SST) and temperate tree-pollen values, while sea level was gradually rising. A decrease in summer insolation at ~1.370 Ma led to an expansion of heathland pollen, reflecting moisture availability under reduced summer evaporation regimes in Portugal (*35*), but steppe-pollen values remained low. Peak interglacial conditions occurred at ~1.366 to ~1.353 Ma, when SSTs reached 20°C and values of deciduous oak and Mediterranean sclerophyll pollen exceeded 40%. Subsequently, benthic and planktic $\delta^{18}O$ values gradually increased, mirrored by a gradual decline in SST and temperate tree-pollen values. The MIS 42 glacial (~1.350 to ~1.338 Ma) contained a series of small, centennial-scale oscillations in $\delta^{18}O_{planktic}$ and SST and an increase in steppe-pollen percentages.

For the second time window, MIS 35 to 34 (Fig. 2, left), all proxies indicate the onset of MIS 35 at ~1.192 Ma, with interglacial conditions extending over two precessional cycles until ~1.154 Ma. The pollen record shows two temperate-tree maxima followed by expansions of heathland, suggesting continued moisture availability, but not an intervening increase in steppe-pollen frequencies. The long MIS 35 (~1.192 to ~1.154 Ma) interglacial was succeeded by a long MIS 34 glacial (~1.154 to ~1.123 Ma), together forming an unusually protracted climate cycle (*15*, *36*) characterized by weak eccentricity forcing (Fig. 2A, left). MIS 34 is marked by the occurrence of four stadials and interstadials from ~1.154 to ~1.127 Ma, similar to the Middle and Late Pleistocene millennial-scale climate variability, including abrupt interstadial onsets and asynchronous phasing of the planktic and benthic $\delta^{18}O$ curves, bearing the fingerprint of the bipolar seesaw (*31*, *33*). A large increase in the abundance of tetra-unsaturated C37 alkenones ($\%C_{37:4}$), indicating the advection of low-salinity polar water masses to the Portuguese margin (*37*, *38*), was accompanied by major decrease in SST, thermocline cooling (*39*), activation of the bipolar seesaw, and maximum expansion of steppe communities at ~1.127 Ma, ushering in a terminal stadial of extreme cold and arid conditions that persisted for 4 kyr before the transition into MIS 33.

Long interglacials and contrasting glacials

Reconstructions from large-mammal remains across the western Paleoarctic indicate alternating open savannah and forested savannah landscapes from ~1.8 to ~1.2 Ma, with increased habitat variability from ~1.2 to ~0.9 Ma; the large diversity of resources, especially along river systems and coastal plains, is considered to have supported hominin dispersal and occupation during both interglacials and glacials (*40*). Our results partly support this view. Both of the interglacial periods that we examined (Fig. 2) were characterized by the persistence of mild and relatively stable conditions with a mosaic of Mediterranean plant communities and open habitats, representing long windows of opportunity for hominin dispersal and occupation. The evidence from the two glacials, however, reveals distinct environmental conditions.

The MIS 42 glacial interval was short (~12 kyr) with subdued centennial-scale SST oscillations (16° to 12°C) and steppe vegetation communities with residual woodland [apart from a brief event with lower SST (9°C) and higher steppe values]. The absence of $C_{37:4}$ suggests minimal advection of cold and fresh polar water masses. The overall environmental conditions correspond to terrestrial reconstructions from Iberia (*27*), indicating relatively mild glacials before 1.2 Ma that would not present barriers to hominin dispersal and occupation. By contrast, MIS 34 was a long glacial (~31 kyr) with a series of pronounced and increasingly colder stadial-interstadial oscillations as low eccentricity allowed the continued growth of ice sheets under the influence of internal climate feedbacks (*41*). This culminated at ~1.127 Ma in a long terminal stadial sustained by meltwater from disintegrating ice sheets, leading to (i) AMOC weakening as suggested by negative $\delta^{13}C_{Cibicidioides}$ anomalies (Fig. 3C) and (ii) cold (SST 5.6°C) and arid (maximum steppe pollen 65%) conditions comparable to the most extreme events of the last 400 kyr (at ~345, ~265, and ~155 ka)

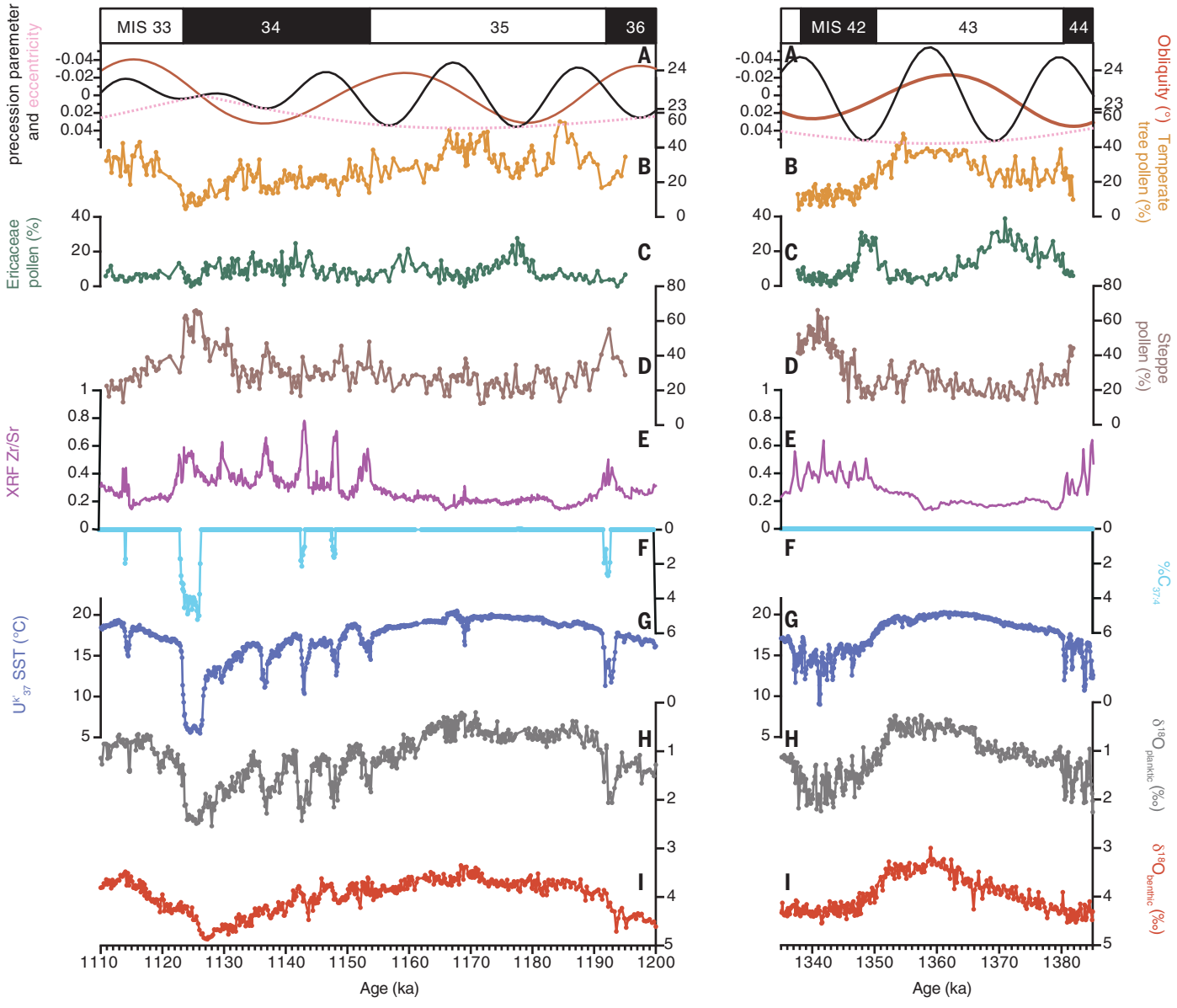

Fig. 2. U1385 paleoclimate records. The figure shows MIS 43 to 42 (right) and MIS 35 to 34 (left). (**A**) Obliquity, eccentricity, and precession parameter (*60*). (**B**) Temperate (Mediterranean+Eurosiberian) tree-pollen percentages. (**C**) Ericaceae (heathland)–pollen percentages. (**D**) Pollen percentages of steppe taxa (Poaceae, *Artemisia*, Amaranthaceae, and *Ephedra*). (**E**) XRF Zr/Sr ratio. (**F**) Abundance of tetra-unsaturated C37 alkenones (%$C_{37:4}$). (**G**) Alkenone-based $U^{K'}_{37}$ SST. (**H**) Planktic $\delta^{18}O$ of *Globigerina bulloides*. (**I**) Benthic $\delta^{18}O$ of *Cibicidioides* spp. Marine Isotope Stages (MISs) are indicated.

recorded on the southwestern Portuguese margin (fig. S2).

The first major glaciation of the Early-Middle Pleistocene Transition is traditionally considered to have occurred during MIS 22, around 0.9 Ma (*21*). However, the Site ODP677 record from the eastern equatorial Pacific shows a shift toward larger $\delta^{18}O_{benthic}$ values in MIS 34 (*15*), implying increasing global ice volume, although this is not as clear in the deconvolved $\delta^{18}O$ of seawater in Site ODP1123 from the southwest Pacific (*16*) (Fig. 3G). In North America, ice from the Keewatin ice center became more extensive during the pre-Illinoian G glaciation, which includes MIS 34 (*42*, *43*). Compilation of sediment volumes and ice-rafted detritus records along the northeast Atlantic continental margin indicates large-scale ice sheet activity in the Kara–Barents-Sea–Svalbard region and more-restricted Fennoscandian and British-Irish ice sheets from ~2.7 to ~1.5 Ma; while an extensive Kara–Barents-Sea–Svalbard ice sheet persisted over the interval ~1.5 to ~0.8 Ma, glacial activity intensified around the North Sea, with ice sheets coalescing during peak glaciations (*44*). More specifically, there is evidence of Fennoscandian and British-Irish ice sheet expansion at ~1.2 to ~1.1 Ma, with the Fedje Till in the Norwegian Channel (*45*, *46*), influx of glaciofluvial deposits from Britain in the central North Sea (*47*), and glacial erratics in the Hattem Beds in the northern Netherlands and adjacent Germany during the Menapian Cold Stage, which has been broadly correlated with MIS 34 (*43*, *47*–*49*).

Considering the interval from 1.4 to 0.8 Ma (Fig. 3, B and E), MIS 34 stands out in the U1385 XRF record (*28*) as an extended period with pronounced Zr/Sr peaks, indicating increases in detrital sediment supply during cold stadials. This compares with results from Site U1308, located near the center of the

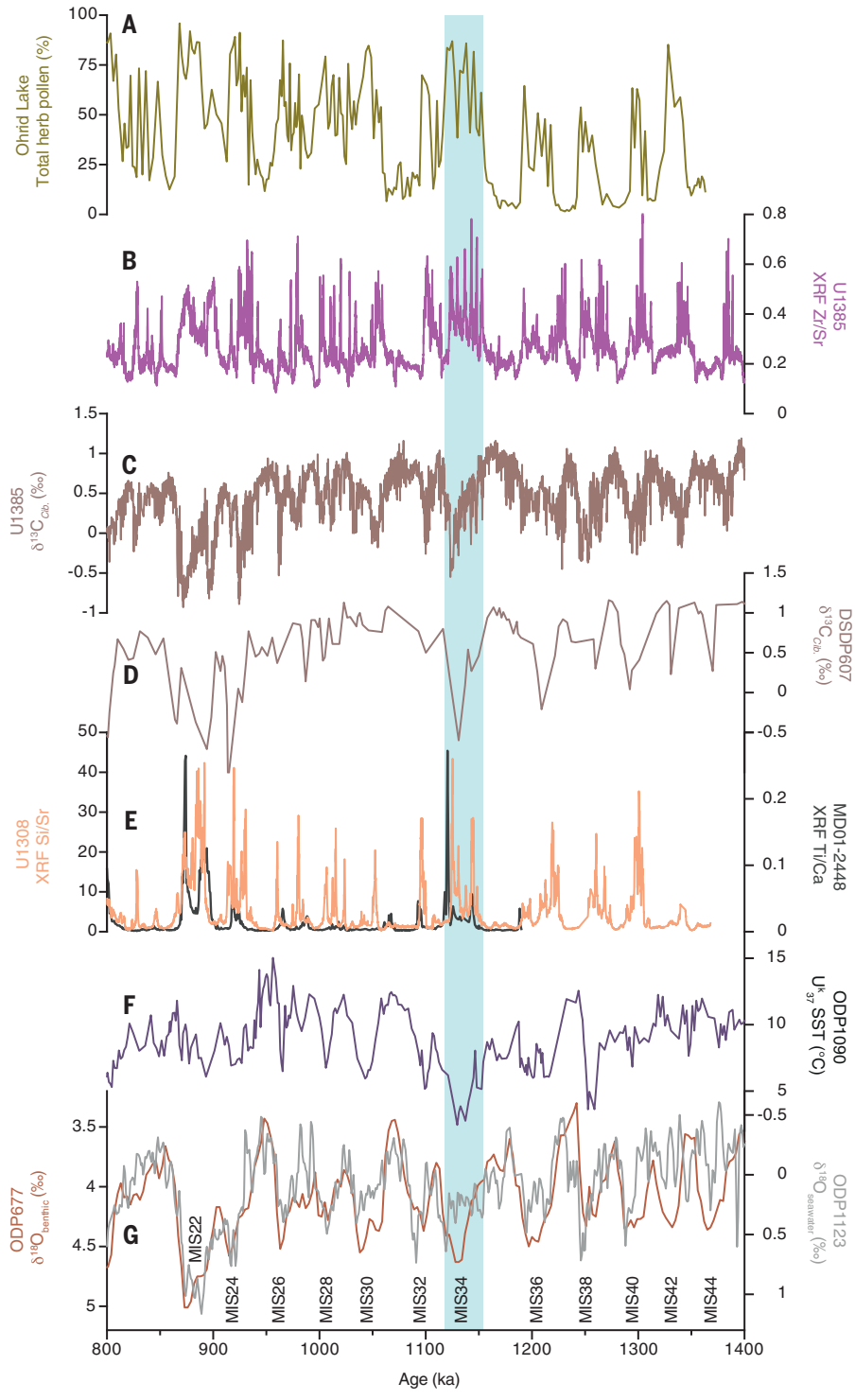

Fig. 3. Comparison of paleoclimate records over the interval 800 to 1400 ka. (**A**) Lake Ohrid (Albania and North Macedonia) total herb pollen percentages (*56*). (**B**) U1385 Zr/Sr record (*28*). (**C**) U1385 benthic $\delta^{13}C$ of *Cibicidioides* spp. (*28*). (**D**) DSDP607 benthic $\delta^{13}C$ of *Cibicidioides* spp. from the North Atlantic (*54*). (**E**) U1308 XRF Si/Sr ratio from the North Atlantic (*18*) and MD01-2448 XRF Ti/Ca ratio from the Bay of Biscay (*50*). (**F**) ODP1090 alkenone-based U^{K}_{37} SST from the South Atlantic (*55*). (**G**) ODP677 benthic foraminiferal $\delta^{18}O$ (orange) from the eastern equatorial Pacific (*15*) and ODP1123 deconvolved $\delta^{18}O$ composition of seawater (gray) from the southwest Pacific (*16*). Marine Isotope Stages (MISs) are indicated.

so-called "ice-rafted detritus belt" of the North Atlantic, which shows high MIS 34 XRF Si/Sr values, reflecting increased delivery of detrital silicate minerals (*18*) of the same order as those from MIS 22. Lithological changes in core MD01-2448 in the Bay of Biscay also show a prominent peak in terrigenous fluxes in MIS 34, suggesting ice-rafted material (*50*), whereas the ice-rafted detritus record from Site ODP983 south of Iceland shows a series of peaks during MIS 34, but whose absolute values do not stand out relative to those of other glacials (*20*).

Previously published North Atlantic SST reconstructions do not show particularly extreme cooling during MIS 34 (fig. S3), but they are of low temporal resolution or do not capture the entire MIS 34 period. Rodrigues *et al.* (*51*) observed that the major cooling events at ~265 and ~155 ka on the southwestern Portuguese margin were amplified relative to those recorded in the central North Atlantic and suggested that the subpolar front may have been deflected southward in the eastern North Atlantic, with the Portugal Current transporting cold water to the vicinity of Site U1385. Climate models simulating the distribution of glacial meltwater in the North Atlantic show the most pronounced negative salinity anomalies on the eastern boundary and along the Iberian Peninsula (*52*), and this is supported by large negative oxygen isotope excursions in deglacial speleothem records from Iberia (*53*), representing meltwater source effects. It is possible that a similar advection of meltwater toward the Portuguese margin occurred during the terminal stadial of MIS 34, as indicated by our $\%C_{37:4}$ record (Fig. 2F, left), which may have contributed to a regional stratification–driven amplification of negative SST anomalies relative to the open North Atlantic. However, prominent MIS 34 changes are also observed beyond the Portuguese margin, suggesting wider-scale impacts, in contrast to the eastern-amplification view: (i) Over the interval 1.4 to 0.8 Ma, the $\delta^{13}C_{Cibicidioides}$ record of Site DSDP607 (*54*) in the central North Atlantic shows the largest reductions in MIS 34 and then MIS 24 and 22, similar to the $\delta^{13}C_{Cibicidioides}$ record of U1385 (*28*), pointing to step changes in deep-ocean circulation (Fig. 3, C and D); (ii) South Atlantic Site ODP1090 has the lowest-recorded SST (2°C, Fig. 3F) of the past 3.5 Myr in MIS 34, together with a major increase in $\%C_{37:4}$, indicating a large expansion of polar waters into the sub-Antarctic region (*55*); and (iii) in southeastern Europe, a pollen sequence of the past 1.36 Myr from Lake Ohrid (*56*) reveals a step change in the intensity and duration of glacials at MIS 34 (Fig. 3A). Whereas earlier glacials were characterized by short expansions of herbs, MIS 34 had sustained high abundances of herbs reaching 85% of total pollen, indicating longer and colder-drier conditions across southern Europe. Taken together,

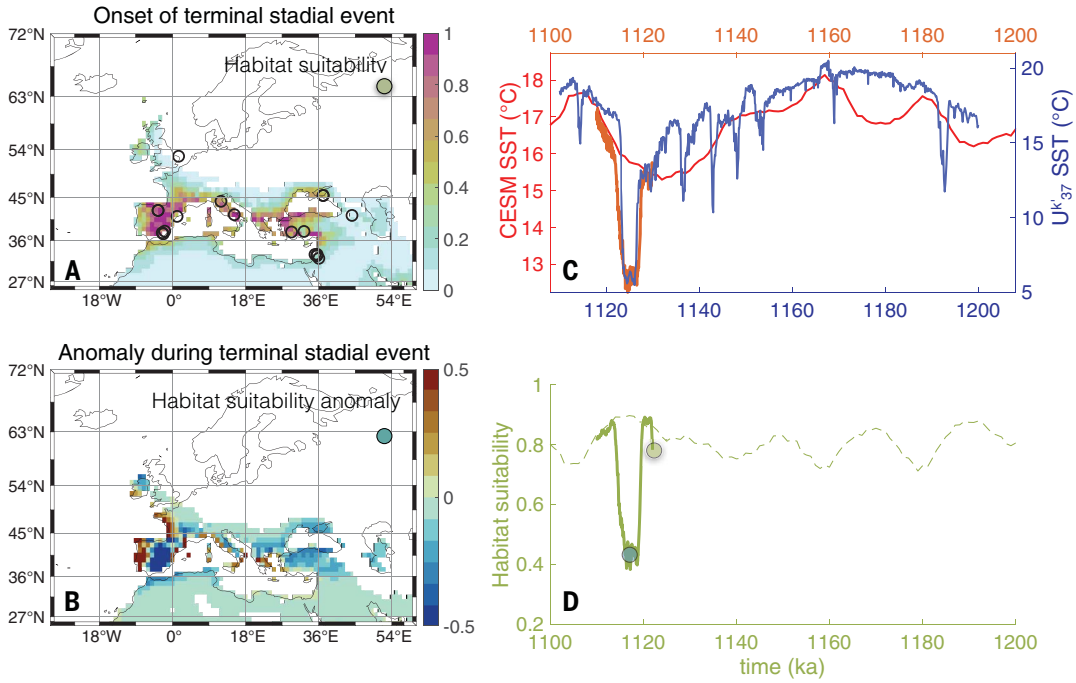

Fig. 4. MIS 34 terminal stadial event impact on early European human habitats. (**A**) Simulated habitat suitability (shaded) for the climate background conditions corresponding to the onset of MIS 34 terminal stadial event conditions (1122 ka CESM1.2 initial conditions), along with locations (circles) of hominin sites included in analysis discussed in text. Habitat suitability values smaller than 0.05 are not displayed. (**B**) Anomaly of habitat suitability during the peak of the MIS 34 terminal stadial event [corresponding to model year 1117 ka (D)]. (**C**) Western Iberian margin SST simulated by the "2Ma" transient CESM1.2 experiment (*34*) (thin red line) and by the freshwater perturbation experiment (thick orange line) (*7*), and alkenone SST from U1385. The offset between the two timescales arises from differences between the U1385 age model (blue) (*7*) and the CESM1.2 age model (red), whose CO_2 forcing before 784 ka is based on the model estimates of (*59*). (**D**) Simulated habitat suitability for "2Ma" (dashed line) and for CESM1.2 MIS34 terminal stadial event simulation (solid olive line) for the western Iberian Peninsula (averaged over 4°W to 0°E, 38°N to 43°N). The timescale in olive corresponds to the model age. The climate envelope model used in (A), (B), and (D) is calculated by using 17 early hominin sites (*7*) and 1000-year mean data of minimum annual temperature and calculated net primary productivity for these sites obtained from the "2Ma" simulation.

the evidence from Europe and the Atlantic suggests an intensification of millennial-scale climate variability and glaciation during MIS 34, which we attribute to its long duration that allowed the expansion of ice sheets, and a subsequent large terminal meltwater release during the deglaciation.

Implications for early hominin occupation in Europe

The picture that emerges for the interval of hominin presence before 1.15 Ma is one of long, stable interglacial conditions and short glacials that would have allowed hominin establishment and occupation. However, the character of glacial periods changed at MIS 34. Its pervasive climatic instability would have placed hominin populations under considerable stress. The likely much-lower carrying capacity of the environment would have challenged small hunter-gatherer bands, compounded by the likelihood that early hominins lacked sufficient fat insulation and the means to make fire, effective clothing, or shelters (*57*, *58*), leading to much-lower population resilience. The terminal stadial event, with an abrupt drop in southwestern Portuguese margin SSTs of ~7°C, represents a drastic climate disruption, which likely affected climate and vegetation patterns across southern Europe with potential implications for early hominin occupation.

To further explore and quantify the possible impacts of this event on early hominin habitability, we conducted a realistic climate model simulation with the Community Earth System Model (CESM), version 1.2, under MIS 34 boundary conditions. Ice sheets were prescribed from a modeling study (*59*), which simulated geographically more-restricted European ice sheets compared with the glacial evidence discussed above. The numerical experiment (*7*) mimics a terminal stadial event by applying anomalous deglacial freshwater forcing to the northern North Atlantic, corresponding to a 23-m sea-level equivalent, which is at the low end of MIS 34 ice-volume estimates (*16*). In response to the freshwater perturbation, the AMOC weakens by about 95%, and SSTs over the west Iberian margin drop by ~3°C—a fraction of the amplitude of the reconstructed temperature anomaly (Fig. 4C). The simulation, therefore, represents a conservative estimate of the climatic changes that occurred during the terminal stadial event. To estimate the corresponding impact on early human occupation of Europe, we developed a climate envelope model (*7*) that links climatic data (minimum annual temperature and net primary productivity) from a transient Pleistocene simulation (*34*) with fossil and archeological evidence of human occupation in Europe and Southwest Asia covering the time period from 2.0 to 0.7 Ma (table S1) (*7*). The climate envelope model is then used to determine how the simulated terminal stadial climate evolution at every grid point impacted habitat suitability. The results (Fig. 4, B and D) show a massive drop in habitat suitability around the Mediterranean by more than 50% around 1.117 Ma on the model timescale (corresponding to 1.125 Ma on the U1385 timescale), which is absent in the transient Pleistocene simulation without the millennial-freshwater perturbation. Climate conditions move far away from the preferred climate niche of early European hominins (Fig. 4B and fig. S4). Lasting for about 4 kyr, this event triggered large-scale shifts in vegetation and ecosystems, as documented by the 45% increase of steppe pollen at Site U1385 and the simulated reduction of 50% in net primary production (fig. S5) over the Iberian Peninsula.

The climatic instability of MIS 34 and the severity of its terminal stadial emerging from this study imply that Iberia, and more generally southern Europe, was depopulated at least once in the Early Pleistocene. Dennell *et al.* (*13*, p. 1514) suggested that the question "When was Europe first colonized?" might be rephrased, "How often was Europe uninhabited after hominins first entered it?" We propose that the question may be further qualified by adding, "and for how long [was Europe uninhabited]?" Although the simulated habitat suitability rebounds following the terminal stadial perturbation (Fig. 4D), Fig. 1 and table S1 hint at a possible longer-lasting hiatus in European and Southwest Asian occupation. If Southwest Asia was depopulated during MIS 34, reoccupation of Europe may have been delayed

until as late as MIS 25, or after the marked glaciation of MIS 22, during MIS 21. This hypothesis can be tested through newly discovered archaeological or hominin sites with robust chronological constraints. If there was the extirpation of hominins in Europe for such an extended period, it implies that repopulation was by *Homo antecessor*, which may have been a more resilient species with evolutionary or behavioral changes that allowed survival under the increasing intensity of glacial conditions.

REFERENCES AND NOTES

1. E. Carbonell *et al*., *Nature* **452**, 465–469 (2008).
2. C. Lorenzo *et al*., *J. Hum. Evol.* **78**, 114–121 (2015).
3. O. Oms *et al*., *Proc. Natl. Acad. Sci. U.S.A.* **97**, 10666–10670 (2000).
4. I. Toro-Moyano *et al*., *J. Hum. Evol.* **65**, 1–9 (2013).
5. J. M. Bermúdez de Castro *et al*., *J. Hum. Evol.* **61**, 12–25 (2011).
6. D. Lordkipanidze *et al*., *Nature* **449**, 305–310 (2007).
7. Materials and methods are available as supplementary materials.
8. T. Mitsui, P. C. Tzedakis, E. W. Wolff, *Clim. Past* **18**, 1983–1996 (2022).
9. J. Garcia, K. Martínez, E. Carbonell, *C. R. Palevol* **10**, 279–284 (2011).
10. J. Rodríguez *et al*., *Quat. Sci. Rev.* **30**, 1396–1412 (2011).
11. Y. Altolaguirre *et al*., *Rev. Palaeobot. Palynol.* **260**, 51–64 (2019).
12. R. Dennell, *J. Hum. Evol.* **45**, 421–440 (2003).
13. R. W. Dennell, M. Martinón-Torres, J. M. Bermúdez de Castro, *Quat. Sci. Rev.* **30**, 1511–1524 (2011).
14. K. MacDonald, M. Martinón-Torres, R. W. Dennell, J. M. Bermúdez de Castro, *Quat. Int.* **271**, 84–97 (2012).
15. N. J. Shackleton, A. Berger, W. R. Peltier, *Trans. R. Soc. Edinb. Earth Sci.* **81**, 251–261 (1990).
16. H. Elderfield *et al*., *Science* **337**, 704–709 (2012).
17. M. E. Raymo, K. Ganley, S. Carter, D. W. Oppo, J. McManus, *Nature* **392**, 699–702 (1998).
18. D. A. Hodell, J. E. T. Channell, J. H. Curtis, O. E. Romero, U. Rohl, *Paleoceanography* **23**, PA4218 (2008).
19. B. Birner, D. A. Hodell, P. C. Tzedakis, L. C. Skinner, *Paleoceanography* **31**, 203–217 (2016).
20. S. Barker *et al*., *Science* **376**, 961–967 (2022).
21. P. U. Clark *et al*., *Quat. Sci. Rev.* **25**, 3150–3184 (2006).
22. H.-A. Blain *et al*., *Quat. Sci. Rev.* **29**, 3034–3044 (2010).
23. C. Sánchez-Bandera *et al*., *Quat. Sci. Rev.* **243**, 106466 (2020).
24. J. Saarinen *et al*., *Quat. Sci. Rev.* **268**, 107132 (2021).
25. J. Ochando *et al*., *Rev. Palaeobot. Palynol.* **304**, 104725 (2022).
26. P. González-Sampériz *et al*., *Rev. Palaeobot. Palynol.* **162**, 427–457 (2010).
27. Y. Altolaguirre, A. A. Bruch, L. Gibert, *Quat. Sci. Rev.* **231**, 106199 (2020).
28. D. A. Hodell *et al*., *Clim. Past* **19**, 607–636 (2023).
29. N. J. Shackleton, M. Chapman, M. F. Sánchez-Goñi, D. Pailler, Y. Lancelot, *Quat. Res.* **58**, 14–16 (2002).
30. P. C. Tzedakis, K. H. Roucoux, L. de Abreu, N. J. Shackleton, *Science* **306**, 2231–2235 (2004).
31. V. Margari *et al*., *Nat. Geosci.* **3**, 127–131 (2010).
32. M. F. Sánchez Goñi *et al*., *Front. Plant Sci.* **9**, 38 (2018).
33. N. J. Shackleton, M. A. Hall, E. Vincent, *Paleoceanography* **15**, 565–569 (2000).
34. A. Timmermann *et al*., *Nature* **604**, 495–501 (2022).
35. V. Margari *et al*., *Geology* **42**, 183–186 (2014).
36. E. L. McClymont, S. M. Sosdian, A. Rosell-Melé, Y. Rosenthal, *Earth Sci. Rev.* **123**, 173–193 (2013).
37. E. Bard, F. Rostek, J.-L. Turon, S. Gendreau, *Science* **289**, 1321–1324 (2000).
38. B. Martrat *et al*., *Science* **317**, 502–507 (2007).
39. A. Bahr *et al*., *Quat. Sci. Rev.* **179**, 48–58 (2018).
40. R.-D. Kahlke *et al*., *Quat. Sci. Rev.* **30**, 1368–1395 (2011).
41. L. E. Lisiecki, *Nat. Geosci.* **3**, 349–352 (2010).
42. R. W. Barendregt, A. Duk-Rodkin, in *Developments in Quaternary Sciences,* vol. 15, *Quaternary Glaciations - Extent and Chronology - A Closer Look*, J. Ehlers, P. L. Gibbard, P. D. Hughes, Eds. (Elsevier, 2011), pp. 419–426.
43. J. Ehlers, P. L. Gibbard, *Quat. Int.* **164-165**, 6–20 (2007).
44. Ø. F. Lien, B. O. Hjelstuen, X. Zhang, H. P. Sejrup, *Quat. Sci. Rev.* **282**, 107433 (2022).
45. H. P. Sejrup *et al*., *Nor. Geol. Tidsskr.* **75**, 65–87 (1995).
46. D. Ottesen, C. L. Batchelor, J. A. Dowdeswell, H. Løseth, *Mar. Pet. Geol.* **98**, 836–859 (2018).
47. J. R. Lee, F. S. Busschers, H. P. Sejrup, *Quat. Sci. Rev.* **44**, 213–228 (2012).
48. W. H. Zagwijn, *Geol. Mijnbouw* **64**, 17–24 (1985).
49. C. Laban, J. J. M. van der Meer, in *Developments in Quaternary Sciences,* vol. 15, *Quaternary Glaciations - Extent and Chronology - A Closer Look,* J. Ehlers, P. L. Gibbard, P. D. Hughes, Eds. (Elsevier, 2011), pp. 247–260.
50. S. Toucanne *et al*., *Quat. Sci. Rev.* **28**, 1238–1256 (2009).
51. T. Rodrigues *et al*., *Quat. Sci. Rev.* **172**, 118–130 (2017).
52. R. Ivanovic *et al*., *Paleoceanogr. Paleoclimatol.* **33**, 807–824 (2018).
53. H. M. Stoll *et al*., *Nat. Commun.* **13**, 3819 (2022).
54. W. F. Ruddiman, M. E. Raymo, D. G. Martinson, B. M. Clement, J. Backman, *Paleoceanography* **4**, 353–412 (1989).
55. A. Martínez-Garcia, A. Rosell-Melé, E. L. McClymont, R. Gersonde, G. H. Haug, *Science* **328**, 1550–1553 (2010).
56. T. Donders *et al*., *Proc. Natl. Acad. Sci. U.S.A.* **118**, e2026111118 (2021).
57. W. Roebroeks, P. Villa, *Proc. Natl. Acad. Sci. U.S.A.* **108**, 5209–5214 (2011).
58. R. T. Hosfield, *Curr. Anthropol.* **57**, 653–682 (2016).
59. M. Willeit, A. Ganopolski, R. Calov, V. Brovkin, *Sci. Adv.* **5**, eaav7337 (2019).
60. J. Laskar *et al*., *Astron. Astrophys.* **428**, 261–285 (2004).
61. V. Margari, D. A. Hodell, J. O. Grimalt, P. C. Tzedakis, Benthic and planktic oxygen and carbon isotopes, alkenone, pollen, and XRF data at IODP 339-U1385 for MIS 34-35 and MIS 42-43 southern Portuguese Margin, PANGAEA (2023); https://doi.org/10.1594/PANGAEA.961070.
62. V. Margari *et al*., MIS34 transient climate model simulation data, Institute for Basic Science ICCP data server (2023); https://doi.org/10.22741/iccp.20230006.
63. V. Margari *et al*., Matlab code for MIS34 human habitat simulation, Institute for Basic Science ICCP data server (2023); https://doi.org/10.22741/iccp.20230007.

ACKNOWLEDGMENTS

We are grateful to M. Casado and Y. Gonzalez (IDAEA-CSIC) for their assistance in the analyses of the alkenones and J. Jadhav for preliminary analysis of Mediterranean climate variability in the CESM1.2 "2Ma" simulation. We thank H.-A. Blain for discussions and M. Irving for drafting fig. S1. The "2Ma" CESM1.2 simulations were conducted on the Institute for Basic Science (IBS) Center for Climate Physics (ICCP) supercomputer Aleph, a Cray XC50-LC system. **Funding:** We gratefully acknowledge financial support from The Leverhulme Trust grant RPG-2014-417 (P.C.T., V.M., and D.A.H.); the Catalan Government, Research Group 2021SGR00986 (J.O.G.); IBS, South Korea grant IBS-R028-D1 (A.T., K.-S.Y., and H.K.); the Human Origins Research Fund (C.B.S.); and the Calleva Foundation (C.B.S., S.A.P., and N.M.A.). **Author contributions:** P.C.T., V.M., and A.T. designed the study. V.M. and P.C.T. wrote the manuscript with contributions from A.T., S.A.P., N.M.A., C.B.S., P.L.G., and D.A.H. V.M., D.A.H., and J.O.G. undertook the pollen, foraminiferal isotope, and alkenone analyses, respectively. S.A.P., N.M.A., and C.B.S. developed the database for the early hominin sites for Europe and Southwest Asia. P.L.G. discussed the glacial geological record. A.T. developed and coded the two-dimensional climate envelope model and downscaled the CESM1.2 data. K.-S.Y. conducted the CESM1.2 "2Ma" simulation and the MIS 34 freshwater perturbation experiments. H.K. conducted a series of isotope-enabled CESM1.2 freshwater perturbation simulations to estimate the overall amplitude of the freshwater forcing for the MIS 34 terminal stadial event. All authors contributed to the ideas in this paper. **Competing interests:** The authors declare that they have no competing interests. **Data and materials availability:** The paleoenvironmental data (*61*) reported in this manuscript are available through PANGAEA. The CESM1.2 climate model data from the MIS 34 water-hosing experiment (*62*) and the MATLAB model code for the habitat suitability model (*63*) used to generate Fig. 4 and figs. S4 and S5 are available on the ICCP data server. The previously published data from the CESM1.2 "2Ma" simulation are available on the OpenDAP and LAS server: https://climatedata.ibs.re.kr/data/hominin-habitats/2ma-transient-climate-simulation-data. The maps in Fig. 4 were generated with M_Map: a mapping package for MATLAB, version 1.4m, available at https://www.eoas.ubc.ca/~rich/map.html. The CESM1.2 code is available at https://www2.cesm.ucar.edu/models/cesm1.2/.

SUPPLEMENTARY MATERIALS

science.org/doi/10.1126/science.adf4445
Materials and Methods
Figs. S1 to S5
Table S1
References (*64–139*)
MDAR Reproducibility Checklist

Submitted 21 October 2022; accepted 22 June 2023
10.1126/science.adf4445

Extreme glacial cooling likely led to hominin depopulation of Europe in the Early Pleistocene

Vasiliki Margari, David A. Hodell, Simon A. Parfitt, Nick M. Ashton, Joan O. Grimalt, Hyuna Kim, Kyung-Sook Yun, Philip L. Gibbard, Chris B. Stringer, Axel Timmermann, and Polychronis C. Tzedakis

Science, **381** (6658), .
DOI: 10.1126/science.adf4445

Editor's summary

Most of what we know about hominin evolution comes from fossil evidence, and these fossils come from a world shaped by climate and ecological dynamics, as ours is today. The ability to estimate these past environments permits us to better understand the forces that shaped our evolution. Using climate models to estimate past environments and spatial distribution models to predict species occurrence, two studies now reveal details about hominin evolution that fossils alone cannot (see the Perspective by Beverly). Looking at habitat overlap for Neanderthals and Denisovans, Ruan *et al*. found patterns of interbreeding between the two that correlate with climate and environmental change in Eurasia. Margari *et al*. have identified a previously unknown climate-driven depopulation of hominins in southern Europe during the early Pleistocene. —Sacha Vignieri